European Journal of Pharmaceutical Sciences 203 (2024) 106912

Contents lists available at ScienceDirect

European Journal of Pharmaceutical Sciences

journal homepage: www.elsevier.com/locate/ejps

A novel sodium caseinate lipid-based auto-emulsifying delivery system to increase resveratrol intestinal permeation: Characterization and in vitro assessment

Andrea Fratter [a,f,*], Andrea Cignarella [b,f], Giovanni Eugenio Ramaschi [a], Adele Papetti [c,f], Vanessa Pellicorio [c], Chiara Milanese [d], Luca Casettari [e,f], Chiara Bolego [a]

[a] Department of Pharmaceutical and Pharmacological Sciences (DSFarm), University of Padova, Italy
[b] Department of Medicine, University of Padova, Italy
[c] Department of Drug Sciences, University of Pavia, Italy
[d] Department of Chemistry, Physical Chemistry Section, University of Pavia and C.S.G.I., Italy
[e] Department of Biomolecular Sciences (DISB), School of Pharmacy, University of Urbino, Italy
[f] Italian Society of Nutraceutical Formulators (SIFNut), Italy

ARTICLE INFO

Keywords:
T-resveratrol
Bioavailability
Sodium caseinate
Lipid-based formulations
Caco-2

ABSTRACT

In recent years, nutraceuticals have emerged as a promising strategy for maintaining health and represent a high-growth market in Italy and across Europe. However, the lack of strict regulations regarding formulation requirements and proof of efficacy raises serious concerns about their poor bioavailability and, consequently, their uncertain health benefits. An emblematic example is t-resveratrol (RES), a cardioprotective stilbene polyphenol that undergoes extensive metabolism in the intestine and liver, resulting in a bioavailability of <1 %.

This manuscript describes a novel technological matrix developed with the primary goal of improving RES oral bioavailability. This technology can be classified as a lipid-based autoemulsifying drug delivery system (LIBADDS), in which RES is thoroughly solubilized in a hot liquid phase composed of lipids and surfactants, and the mixture is further adsorbed onto a powder composed of polysaccharides and sodium caseinate (N_aC), along with inert excipients, and then compressed.

In this study, NaC was used for the first time to trigger pancreatin-mediated hydrolysis of an enteric-coated tablet, allowing micellar delivery of RES to the small intestine. The RES-containing tablets were characterized via differential scanning calorimetry (DSC) and X-ray diffraction (PXRD). The digested formulation, with simulated gastric and enteric fluids, was dimensionally assessed via dynamic light scattering (DLS). Finally, calculations of the bioaccessible fraction, dissolution tests, and in vitro permeability experiments using Caco-2 cell monolayers were carried out to preliminarily define the overall efficiency and applicability of this new technology in improving RES intestinal permeability.

1. Introduction

RES is a polyphenolic stilbene extracted from several parts of plants, particularly from the seeds and skin of *Vitis vinifera* and the roots of *Poligonum cuspidatum*. This molecule has attracted the interest of pharmacologists and clinicians over the last 3 decades because of its well-proven cardioprotective effects (Hung et al., 2000; Wu and Hsieh, 2011; Bertelli and Das, 2009), its ability to prevent osteopenia and cognitive decline during menopause (Wong et al., 2020; Thaung Zaw et al., 2021) and its ability to modulate caspase and sirtuin enzyme activity (Miki et al., 2012; Gertz et al., 2012). Despite good intestinal bioaccessibility, as reported by Walle, RES bioavailability remains low and limited in humans (Walle, 2011; Walle et al., 2004). In particular, RES is extensively metabolized in liver microsomes and intestinal cells by phase II enzymes such as UDP-glucuronyl transferase. As a consequence, RES glucosides and sulfates are the main metabolites found in blood (Francioso et al., 2014; Vitaglione et al., 2005; Vesely et al., 2021). For these reasons, novel technological approaches to improve RES bioavailability are strongly needed (Amri et al., 2012a). The delivery of small lipophilic substances represents a challenge from a

* Corresponding author at: Department of Pharmaceutical and Pharmacological Sciences, University of Padova, Italy.
E-mail address: andrea.fratter@phd.unipd.it (A. Fratter).

https://doi.org/10.1016/j.ejps.2024.106912
Received 1 August 2024; Received in revised form 11 September 2024; Accepted 14 September 2024
Available online 18 September 2024

technological and pharmacological point of view, given the need to make them dispersible in water-based intestinal fluids to be absorbed. From this perspective, novel approaches aimed at releasing lipophilic active molecules in emulsified or micellized forms in the small intestine are attracting increasing attention and technological efforts.

Several technological approaches have been investigated in the attempt to improve RES bioavailability. In particular cyclodextrin encapsulation, nanoemulsions, enteric-coated matrixes (Salla et al., 2024; Smoliga and Blanchard, 2014; Amri et al., 2012b). All these technological tools affect RES water solubility and intestinal micellization, but they do not modify, except to a minimal extent RES biotransformation, extrusion and permeation phenomena through the intestinal cell in its unmodified form. Regarding the concomitant use of piperine, an alkaloid extracted from *Piper nigrum* to inhibit intestinal UDP-glucuronosyltransferase, published studies deny its real effectiveness in reducing the presystemic metabolism of RES. In any case, the described dosages are incompatible with human use (Johnson et al., 2011; Bailey et al., 2021). Finally, the sublingual approach, that theoretically should allow RES to reach systemic circulation in unmodified form, has not yet found sufficient scientific evidences to validate its effectiveness and foster its application (Di Prima et al., 2021). Among others, self-emulsifying drug delivery systems (SEDDSs) and lipid-based auto-emulsifying drug delivery systems (LiBADDSs) are widely described and cited in specialized literature (Zhu et al., 2020; Rani and Radha, 2021; Salawi, 2022; Pandey and Kohli, 2018; Cerpnjak et al., 2013; Bu et al., 2017). These delivery systems, in fact, foster the dispersion of lipophilic or poorly soluble active substances in the form of prompt emulsions or micellar dispersions just in contact with the gastroenteric fluids. This results in remarkably improved bioaccessibility and, at the same time, provides some protection towards enteric presystemic metabolism. Several research groups are attempting to deliver lipophilic small molecules from enterocytes to lymphatic capillaries to prevent portosystemic metabolism, which substantially reduces bioavailability, as mentioned for RES. This approach relies on the incorporation of small lipophilic molecules into chylomicrons such as long-chain unsaturated fatty acids (Trevaskis et al., 2008; Zhang et al., 2024; Acta Pharmaceutica Sinica 2021; Yáñez et al., 2011) and hydrophilic surfactants such as polysorbate 80 (PS80) (Sangsen et al., 2016; Acharya et al., 2013a). We describe here a novel RES-containing LiBADDS, in which a combination of N_aC, conjugated linoleic acid (CLA) and PS80, in a precise weight ratio with respect to each other, improved RES intestinal permeability in unmetabolized form (patent application submitted n°102024000015469: co-ownership between Laboratorio della Farmacia SPA-University of Padova). The main objective of this work was to develop a novel LiBADDS in which N_aC plays a dual role as both an enteric-coated agent and a surfactant in the duodenum. This technological hypothesis is based on studies by Van Skype and Wang showing that N_aC is coagulated at low pH and not by pepsin (Van Slyke and Bosworth, 1913; Wang et al., 2018). Tablets manufactured by physical absorption of the lipid-based phase containing RES into the N_aC powder and inert excipients underwent in vitro tests to assess gastric resistance and micellar dispersion in both fasted-state simulated gastric fluid (FSSGF) and fasted-state simulated intestinal fluid (FaSSIF) in the presence of pepsin and pancreatin, respectively. A correlation between the N_aC/PS80 ratio and disaggregation time was established in the presence and absence of enzymes with and without the LiBADDS phase. Differential scanning calorimetry (DSC), PXRD, and DLS analysis of LiBADDS dispersion in FaSSIF and dissolution tests were carried out to characterize the features and release kinetics of this new technology. Finally, a permeation test with Caco-2 cell monolayers was carried out to assess whether LiBADDS technology affects RES intestinal permeation and whether the excipients affect ATP-binding cassette transporter activity in extruding RESs from enterocytes.

2. Materials and methods

2.1. Materials

Compritol 888 Ato (Glyceryl dibehenate) was purchased from Gattefossè (Milan, Italy), Veremul T 80 (Polysorbate 80) was purchased from Eigenmann-Veronelli (Milan, Italy), and Tocopherol and Tonalin A 80 (conjugated carboxylic linoleic acid) were purchased from BASF (Cesano Maderno, MB, Italy). EMUL AC (sodium caseinate), magnesium stearate and citric acid were purchased from Faravelli SPA (Milan, Italy). Resveratrol was purchased from Suissenutra (Monza, Italy). A Comprez (anhydrous calcium phosphate) and Ceolus KG 802 (microcrystalline cellulose) were purchased from Seppic SRL (Milan, Italy); amorphous silica was purchased from Brenntag (Milan, Italy). FaSSIF and FSSGF were purchased from Biorelevant (London, United Kingdom); pepsin from porcine gastric mucosa, pancreatin 4X USP, methanol and ethyl acetate were purchased from Merck (Rome, Italy).

2.2. Preparation of resveratrol-containing sodium caseinate-based tablets

A total of 125 g of EMUL AC, 20 g of RES, 580 g of Ceolus KG802 (microcrystalline cellulose), 25 g of amorphous silica, 225 g of A Comprez (Anhydrous Dibasic Calcium Phosphate) and 25 g of magnesium stearate were weighed, mixed with a mechanical stirrer at 300 rpm for 10 min and then mixed with a V-shaped mixer (MSE PRO Lab Scale V-shaped Mixer) for an additional 10 min. The powder mixture was sieved with a 40-mesh stainless steel sieve and further compressed to obtain 1.0 g tablets. Tablets have undergone quality control for unique pharmaceutical forms, such as hardness, flowability, friability and abrasion. The same method was employed to fabricate tablets containing increasing amounts of N_aC (Table 1). The tablets were loaded with the same quantity of excipients, and the difference in N_aC content was restored with microcrystalline cellulose.

2.3. Preparation of resveratrol-containing LiBADDS tablets

Tablets were prepared using different relative amounts of N_aC, PS80 and RES while maintaining constant glyceryl dibehenate (GB) and CLA contents. Among these, only 3 fully passed the quality control and overall industrial feasibility assessment (Table 2).

Veremul T80, Compritol E ATO, Tonalin A 80 and tocopherol were mixed in a 500 ml glass Becher and heated to 85 °C to achieve a clear oily phase. RES was weighed and poured into the hot oily phase under gentle mechanical stirring. The mixture was stirred at 85 °C with a thermostatic probe until RES was completely solubilized. After that, the hot oily phase was rapidly poured into a stainless-steel vessel containing EMUL AC under rapid mixing to achieve a uniform wet powder. When the coarse powder reached 25 °C, the remaining excipients, including calcium phosphate, magnesium stearate, microcrystalline cellulose and amorphous silica, were mixed to obtain 1000 g of final RES-containing LiBADDS powder. The powder was further sieved and compressed to obtain the final tablets. Tablets have undergone quality control for unique pharmaceutical forms, such as hardness, flowability, friability and abrasion (Table 3).

2.4. Preparation of unformulated RES-containing tablets

Five grams of RES, 25 g of amorphous silica, 225 g of A Comprez (Anhydrous Dibasic Calcium Phosphate), 25 g of magnesium stearate and Ceolus KG802 (microcrystalline cellulose) up to 1000 g were weighed, mixed with a mechanical stirrer at 300 rpm for 10 min and then mixed with a V-shaped mixer (MSE PRO Lab Scale V-shape Mixer) for an additional 10 min. The powder mixture was sieved with a 40-mesh stainless steel sieve and further compressed to obtain 1.0 g tablets. Tablets have undergone quality control for unique pharmaceutical forms, such as hardness, flowability, friability and abrasion.

Table 1
Composition of N_aC-based tablets. EMUL AC: sodium caseinate.

Formulation									
	1	*2*	*3*	*4*	*5*	*6*	*7*	*8*	*9*
RES (g)	0.020	0.020	0.020	0.020	0.020	0.020	0.020	0.020	0.020
EMUL AC (N_aC) (g)	0.125	0.150	0.200	0.225	0.250	0.375	0.437	0.500	0.625

Table 2
Qualitative composition of RES-LiBADDS tablets per tablet. N_aC, EMUL AC, sodium caseinate; GB, Compritol 888 ATO, glyceryl dibehenate; CLA, Tonalin A 80, conjugated linoleic acid; PS80, Veremul T 80, polysorbate 80.

	RES LiBADDS 013	RES LiBADDS 015	RES LiBADDS 017	RES LiBADDS 019
RES (g)	0.010	0.010	0.010	0.005
EMUL AC (N_aC) (g)	0.280	0.300	0.500	0.390
VEREMUL T 80 (PS 80) (g)	0.035	0.025	0.050	0.045
COMPRITOL 888 ATO (GB) (g)	0.010	0.010	0.010	0.005
TONALIN A 80 (CLA) (g)	0.005	0.005	0.005	0.002
Ratio (PS80/RES)	3.5	2.5	5.0	9.0
Ratio N_aC /(PS80/RES)	0.080	0.120	0.100	0.043
Industrial feasibility	Yes	yes (with some technical limitations)	yes (with some technical limitations)	yes (with some technical limitations)

2.5. Simulated digestion of RES-based, RES- N_aC-based, and RES-based LiBADDS tablets

Six RES-based (prepared as described in Section 2.2), RES-N_aC-based (prepared as described in Section 2.3), and RES-based LiBADDS (prepared as described in Section 2.4) tablets were placed in the disaggregation device (Sotax, disaggregation apparatus DT50), according to the European Pharmacopoeia (European Pharmacopoeia, 2024). The chamber was filled with 800 mL of FSSGF at pH = 1.6. The test was carried out over 2 h at 37 °C in the presence and absence of pepsin (2000 U/mL) (Brodkorb et al., 2019; Mudie et al., 2014; Vrbanac et al., 2020). The same test was also carried out to evaluate the gastric resistance of RES-N_aC-based tablets containing increasing amounts of N_aC. The tablets were further tested using a novel device mimicking the mechanism of human gastroenteric movements in the presence of FSSGF-pepsin, as described in Section 3.1. The surface of the tablets after disaggregation in FSSGF was observed under an optical microscope (Celeston Tetraview, Touch screen 40–400 X).

A total of 400 mL of each obtained FSSGF dispersion was added to 400 mL of double-concentrated FaSSIF according to the two-stage dissolution experiment described by Geboers et al. (2016). The pH was adjusted to 6.5 with sodium bicarbonate, and 10 mg/mL pancreatin 4X USP was added to the mixture. The dissolution was carried out until the tablets were completely disaggregated both in the presence and absence of pancreatin. When dissolution was completed, aliquots of 20 mL of each sample were taken, centrifuged at 6000 rpm and 37 °C for 15 min and analysed by HPLC-DAD to quantify the RES isomers (*cis* and *trans*) both in the supernatant and in the pellet.

2.6. Differential scanning calorimetry (DSC) characterization of the LiBADDS phase

The samples were analysed on a Mettler Toledo DSC 3 Star System (Milan, Italy) via STAR^e software version 16.40 for data analysis. Aluminium pierced crucibles were loaded with a suitable amount of powder to obtain 2 mg, accurately weighed, of sample. The heating programme included a temperature ramp of 10 °C/min from 30 °C to 160 °C under nitrogen flux (50 mL/min).

2.7. PXRD characterization of the LiBADDS phase

For powder PXRD measurements, a Bruker D2 Phaser diffractometer (Bruker, Mannheim, Germany) with a Cu-Kα source (λ = 1.54 Å) was used. The system works with a 300 W low-power X-ray generator (30 kV at 10 mA). Steel sample holders with a capacity of approximately 300 µL were equipped with cylindrical gearboxes in polyvinylidene fluoride (PVDF) to reduce the capacity to approximately one third. The conditions used for the measurements were as follows: 2θ angles from 5° to 35°, 0.02° θ increments, and a time step of 0.6 s.

2.8. Determination of the LiBADDS dispersed phase size in digestive fluids via DLS

The DLS technique was applied on a Malvern Zetasizer Nano Series (Nano-S). The size range was between 0.6 nm and 6.0 µm. The measurements were run at a temperature of 25 °C°C via disposable polystyrene cuvettes (10 × 10 × 45 mm). The dispersing medium was water (diffraction index: 1.330, viscosity: 0.8872 cp). The sample volume required to perform the analysis was 1 mL. The RES LiBADDS dispersion in FaSSIF was previously filtered with a 0.450 µm cellulose acetate membrane to separate the insoluble material (excipients) derived from tableting and finally diluted 1:100.

2.9. Assessment of the RES bioaccessible fraction after simulated in vitro digestion

Twenty millilitres of the supernatants obtained as described in Section 2.5 were mixed with an equal volume of ethyl acetate to break down

Table 3
Main physical parameters of tablets containing N_aC and LiBADDS.

	Hardness (N) (threshold for acceptability 90 N)	Flowability (angle of repose, Hausner's ratio-Carr's Index)	Friability (100 RPM/25 RPM/min) 10 tablets	Abrasion (100 RPM/25 RPM/min) 10 tablets
N_aC tablets	>120	Good	<1 %	<1 %
RES LiBADDS 013	60–70	Fair	<1 %	<1 %
RES LiBADDS 017	70–80	Poor	<1 %	<1 %
RES LiBADDS 019	90–100	Passable	<1 %	<1 %

the micelles and extract RES in both the *cis* and *trans* isomers. The organic phase was then dried in a rotary evaporator and replaced with 2 ml of methanol. The methanolic solution was then analysed with HPLC-DAD. The pellets collected at the bottom of the vials as described in Section 2.5 were mixed with the minimal volume of methanol and further analysed via HPLC-DAD. The bioaccessible fraction (BF) of RES was calculated according to Eq. (1):

$$BF = (RES_{mic} / RES_{tot}) * 100 \quad (1)$$

where RES_{mic} is the fraction of RES encapsulated in the supernatant mixed with micelles and RES_{tot} is the total amount of RES loaded in the tablets as recovered by HPLC-DAD analysis.

2.10. Dissolution test

In vitro release of RES from RES LiBADDS 019 tablets was carried out in FaSSIF in the presence of pancreatin (10 mg/mL) (900 mL, pH = 6.5) at 37 °C ± 0.5 C° and 100 rpm via a USP II dissolution test apparatus (P Dissolution Test Apparatus, Model 1912, SunShine Scientific, New Delhi, India). A 10-mL aliquot was taken from the dissolution medium at specified time intervals (15′, 30′, 45′, 60′, 90′, 120′ and complete dissolution) and replenished immediately with the same volume of FaSSIF+pancreatin at 37 °C. The liquid aliquots were then centrifuged at 6000 rpm for 15 min. Both the supernatants and pellets were further subjected to chromatographic analysis (HPLC-DAD) after extraction with an equal volume of ethyl acetate, the organic phase was dried with rotavapor, and the dry residue was finally redissolved with 2 ml of MeOH.

2.11. HPLC–DAD analysis

An Agilent 1200 HPLC system (Waldbronn, Germany) equipped with a mobile-phase online degasser, a quaternary pump, an autosampler, a column heater, and a diode array detector (DAD) was used for the analyses. The separation was performed according to Sessa et al. (2014) with slight modifications using a Gemini® C18 analytical column (150 × 2.0 mm i.d., 5 µm, Phenomenex, Torrance, CA, USA), which was heated at 30 °C. The mobile phase consisted of methanol acetic acid:water 45:5:50 (v/v) (A) and methanol:acetic acid 98.8–1.2 (v/v) (B), and the gradient elution started with 100 % A, reaching 100 % A after 6 min 90 % A, and after 1 min 0 % A. After 30 s at 0 %A, the column was then reconditioned for 2.5 min. The flow rate was 0.3 mL/min, and 2 µL of sample was injected. The detection wavelengths were 310 nm for trans-resveratrol and 280 nm for cis-resveratrol. The quantification of trans-resveratrol was performed via the external standard method. A trans-resveratrol calibration curve in the range of 0.5–150 µg/mL was constructed (R^2 0.9997). The standard curve was constructed by diluting resveratrol in MeOH to obtain final concentrations of the calibrator solutions in the range of 0.5–150 µg/mL (the curve is available in the Supplementary Materials section, Fig. S1).

2.12. Cell culture materials

High-glucose Dulbecco's modified Eagle's medium (DMEM), Roswell Park Memorial Institute (RPMI) 1640 medium, Hanks' balanced salt saline (HBSS), nonessential amino acids (NEAA), L-glutamine, penicillin–streptomycin mixture, and Lucifer yellow were purchased from Sigma–Aldrich (St. Louis, MO, USA). Caco-2 human colorectal adenocarcinoma cells (ATCC® HTB-37™) were purchased from ATCC (Manassas, VA, USA). The CellTiter 96® Aqueous One Solution Cell Proliferation Assay (MTS) was purchased from Promega (Madison, WI, USA). Transwell® inserts were purchased from Millipore (Burlington, MA, USA). Fetal bovine serum (FBS) was purchased from Euroclone (Milan, Italy).

2.13. Caco-2 cell culture

Human adenocarcinoma Caco-2 cells (ATCC, HTB-37™) were seeded in adhesion flasks in complete medium (high-glucose DMEM, 10 % heat-inactivated FBS, 1 % nonessential amino acids, 4 mM L-glutamine and 1 % penicillin/streptomycin mix) at a density of 2×10^3 cells/cm^2 and maintained at 37 °C and 5 % CO_2 in a humidified incubator. The cells were subcultured by trypsinization every 7 days when 80–90 % confluent and seeded at a density of 2000 cells/cm^2. The medium was changed every other day.

2.14. In vitro model of the intestine

The intestinal absorption of RES contained in RES LiBADDSs and unformulated RES formulations was assessed via a model of the human enteric epithelium in vitro on the basis of Caco-2 cells organized in a functional monolayer placed in Transwell inserts. Transwell inserts are characterized by two compartments separated by a microporous membrane: apical or luminal and basolateral or serosal. Monolayers of Caco-2 cells growing on the surface of microporous membranes consist of polarized cells with morpho-functional features typical of human enterocytes, such as the presence of microvilli, tight junctions, and efflux ATP-binding cassette (ABC) transporters such as P-glycoprotein (P-gp) (Artursson et al., 2001; Schreck and Melzig, 2018). Briefly, Caco-2 cells were seeded at a density of 1.5×10^5 cells/cm^2 on 1 µm pore size Transwell® polytetrafluoroethylene inserts and allowed to mature and differentiate for 21 days. Absorption experiments were performed on day 21 post-seeding.

2.15. Enteric cell viability

The effects of the digested formulations on the viability of the enteric epithelium were assessed through a dose–response curve. After digestion, as described in Section 2.5, the BFs of both RES LiBADDS 019 and unformulated RES contained in the six tablets disaggregated in digestive fluids were diluted in FaSSIF to obtain the BF of RES contained in 1 tablet. Increasing dilutions of the tablet BFs in FaSSIF were added to the apical compartment of the Caco-2 monolayers, while HBSS enriched with 1 % BSA was added to the basolateral compartment. As a negative control, FaSSIF without RES was used. After 3 h of incubation, the viability of the enteric epithelium was assessed via the 3-(4,5-dimethylthiazol-2-yl)−5-(3-carboxymethoxyphenyl)−2-(4-sulfophenyl)−2H-tetrazolium (MTS) assay, according to the manufacturer's instructions. The MTS assay is based on the reduction of the MTS tetrazolium compound from vital cells in the presence of phenazine methosulfate to generate the colored compound formazan, which can be titrated by measuring the absorbance at 490 nm with a microplate reader (Synergy4, Biotek). Cell viability (%) was expressed as the ratio of the absorbance in the treated groups to that in the control (untreated) group.

2.16. Integrity of barrier function in the enteric epithelium

Barrier integrity was assessed by measuring the transepithelial electrical resistance (TEER) of the monolayer with an ERS2 Voltmeter 273 (Millipore) equipped with a chopstick electrode and by measuring the permeability of Lucifer yellow (LY), a polar tracer unable to permeate intact tight junctions. Permeability was measured by adding 0.2 mL of a 100 µg/mL solution of LY in HBSS to the apical compartment and 0.6 mL of HBSS to the basolateral compartment. After a 1-h incubation, the basolateral fractions were collected, and the fluorescence intensity at 490 nm was measured via a microplate reader (Synergy4, Biotek). To convert the rate of fluorescence to the LY concentration (µg/mL), a calibration curve was generated in the range from 0 to 6.25 µg/mL (fluorescence values between 100 and 12.5 µg/mL were not considered since the fluorescence signal at these concentrations tends to

be saturated).

2.17. Measurement of resveratrol permeation through the enteric epithelium

Once the barrier integrity was verified, the cells were treated with the solution under examination to check apical-to-basolateral (A-B) and basolateral-to-apical (B-A) passages. In the first case, the medium in the apical compartment was replaced with 400 μL of the higher nontoxic dispersion of RES LiBADDS 019 and unformulated RES in digestive fluids (diluted, if necessary, in FaSSIF), whereas in the basolateral compartment, it was replaced with 600 μL of 1X HBSS (1 % BSA). In the second case, 600 μL of the higher nontoxic dispersion of RES LiBADDS 019 and unformulated RES in digestive fluids (diluted, if necessary, in FaSSIF) was applied in the basolateral compartment, whereas 400 μL of 1X HBSS (1 % BSA) was applied in the apical compartment. RES-free FaSSIF was used as a control. The plate was incubated for 3 h, with TEER measured every hour for each well, and 100 μL samples were taken from the basolateral compartment for A–B passage and from the apical compartment for B-A passage to be analysed by HPLC to determine the amount of permeated substance during treatment. This volume was replenished with 1X HBSS (1 % BSA). At the end of the treatment, i.e., after three hours, a sample was taken from each well in both compartments. To verify the integrity of the monolayer after treatment, the LY test was performed again. Finally, the TEER was also checked 24 h after treatment.

The apparent permeability coefficient (P_{app}, cm/min) was calculated without linear model fitting according to the following non-sink Artursson Eq. (2) (Hubatsch et al., 2007; Tavelin et al., 2002):

$$CR_{(t)} = [M/(V_D + V_R)] + (CR_0 - [M/(V_D + V_R)])e\left(-P_{app}A(1/V_D + 1/V_R)t\right)(nonlinearcurvefittingequation) \quad (2)$$

where V_D is the volume of the donor compartment, V_R is the volume of the receiver compartment (cm^3), A is the area of the membrane (cm^2), M is the total amount of substance in the system, $CR_{(0)}$ is the concentration of the substance in the receiver compartment at the start of the time interval, and $CR_{(t)}$ is the substance concentration at time t measured from the start of the time interval.

The apparent permeability coefficient (P_{app}, cm/min) was calculated in the case of steady-state flux according to Eq. (3):

$$P_{app} = (dQ/dt) * 1/(A * C_0) \quad (3)$$

where dQ/dt is the steady-state flux of the molecule transported through the monolayer during incubation (mM/min), A is the area of the membrane (cm^2), and C_0 is the initial concentration of LY in the apical compartment (mM).

The percentage of RES permeation for both the unformulated RES and RES-LiBADDS was calculated according to the following equation:

$$\%RES_{perm} = BF * RES_{A-B(Caco-2)} * 100 \quad (4)$$

2.18. Statistical analyses

All the data reported are expressed as the means ± SDs of three independent experiments. All the biological experiments were carried out in duplicate. Student's *t*-test was used within pairs of experiments via a one- or two-tailed test. Analysis of variance was performed with one-way ANOVA. *A post hoc* Dunnett test was also performed. $p < 0.05$ was considered to indicate statistical significance. Analyse.it (in Microsoft Excel) software was used for all the analyses.

3. Results and discussion

A novel RES-based LiBADDS containing sodium caseinate (N_aC), conjugated linoleic acid (CLA), and PS80 was investigated for RES bioaccessibility and compared with a RES-N_aC-based formulation. NaC is the soluble sodium salt of a milk protein that is widely used in the food industry and pharmaceutical technology to develop nanoemulsions, nanomicelles and other delivery systems owing to its unique physicochemical properties and versatility of use (Acharya et al., 2013b; Madan et al., 2020; Yuan et al., 2021). NaC possesses amphiphilic features due to its carboxylic groups and proteinaceous core, which makes it particularly suitable as an emulsifying agent. CLA is an unsaturated long-chain fatty acid that can be salified at neutral pH values, thereby acting as an ionic surfactant. In LiBADDS, N_aC plays a dual role as a resistance agent because it is coagulated at low pH but not by pepsin or a surfactant in the duodenum. PS80 is a nonionic hydrophilic surfactant widely used in the pharmaceutical, food and cosmetic industries as an emulsifier and solubilizing agent.

To evaluate RES bioaccessibility, RES-N_aC -based and RES-based LiBADDS tablets were subjected to a simulated digestion process consisting of two phases, gastric and intestinal.

3.1. Tablets physical parameters

Only RES LiBADDS 019 tablets fully overcame all the physical tests for solid pharmaceutical forms according to Pharmacopoeia.

3.2. Effects of simulated digestion conditions on RES- N_aC-based and RES-based LiBADDS tablets

With respect to the effect of simulated gastric conditions on RES-N_aC -based tablets, in the presence of pepsin on the tablet surface, fractures, as evident from the images obtained via an optic digital microscope, which also revealed a generally jagged surface appearance of the tablets (Fig. 1A and C), except for those containing 125, 150, 200 and 225 mg N_aC, thus indicating an effect of the enzyme on the surface morphology.

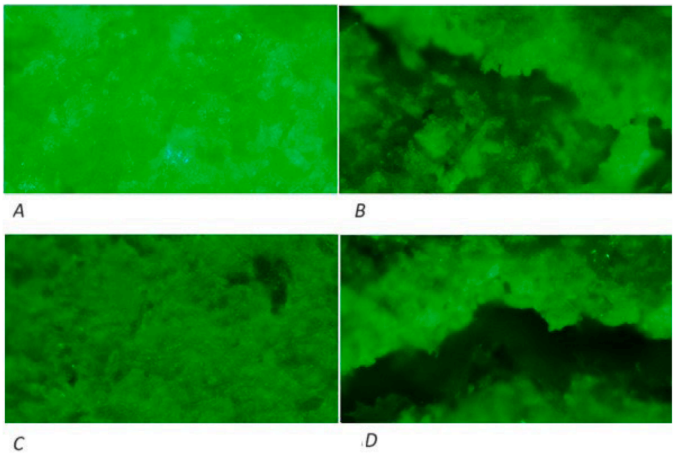

Fig. 1. Optical microscope (40X). Disruption of the surface of RES-LiBADDS-containing tablets (*D*) and N_aC-containing tablets (*B*) in FSSGF/pepsin medium. The surfaces of the tablets disaggregated in FSSGF in the absence of pepsin did not show any breaks (*A, C*). This is likely due to the hydrolytic activity of pepsin on N_aC on the tablet surface.

In fact, this feature was completely absent in the tablets disaggregated in the gastric medium without pepsin. This suggests that pepsin changed the tablet surface morphology by partially hydrolysing N_aC and generating breaks.

With respect to RES-based LiBADDS tablets, their feature in simulated gastric fluid was similar to that registered for RES-N_aC-based tablets, and in this case, the optic microscope analysis highlighted the presence of fractures when disaggregated in the presence of pepsin (Fig. 1B and D). Interestingly, although PS80 could lead to early tablet disaggregation due to its ability to attract water, the overall structure appeared to be resisted. In contrast, RES-based tablets completely disaggregated in FSSGF in 20 - 35 min.

The tablets were shown to resist simulated gastric conditions both in the presence and absence of pepsin, and no disaggregation was registered not only when the European Pharmacopeia test was applied but also when a novel, patented device that mimics gastroenteric movements was used (Fig. 2, Movie 1 is available in the Supplementary materials Section).

Furthermore, this new device allows exploration of the tablet disaggregation process in real time by introducing a probe inside the gastric chamber (Movie 2 is available in the Supplementary materials Section). Therefore, these results suggest that pepsin can interact with N_aC on the tablet surface but is not able to hydrolyse N_aC in the tablet inner core, thus preserving its overall integrity. The gastroresistant RES-N_aC -based tablets (containing 250, 375, 437.5, 500 and 625 mg N_aC) in FaSSIF disaggregated both in the presence and absence of pancreatin, showing a linear inverse correlation ($R^2 = 0.9998$) between the average disaggregation time and the N_aC content in the presence of pancreatin. An increase of 125 mg N_aC in the tablet led to a 22 min reduction in disaggregation time, thus suggesting a “sustained release-like” behavior mediated by N_aC that is triggered in vivo by enteric proteases (Fig. 3).

On the other hand, by plotting the disaggregation time of tablets in the absence of pancreatin against the N_aC content, a direct correlation was observed, and a remarkable increase in the disaggregation time was evident (Fig. 4).

This finding confirms the role of pancreatin in cleaving N_aC molecules, hence accelerating tablet disaggregation. Furthermore, the pseudo-neutral pH of the FaSSIF disaggregation medium, while it was able to maintain N_aC in its ionic form in solution (pH>pKa of N_aC), was not sufficient to provide faster disaggregation. This could be due to the occurrence of N_aC salification on the tablet surface but not throughout its inner core. Therefore, the presence of pancreatin can be considered crucial to promote disaggregation.

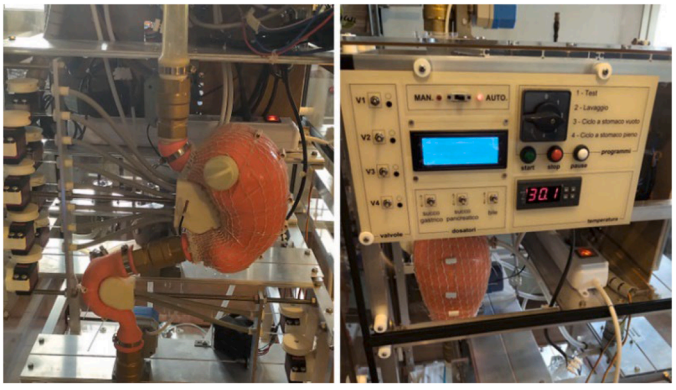

Fig. 2. (Gastromachine) Device simulating gastroenteric movements. This machine improves the reliability of disaggregation tests by replicating gastric movements. This approach is useful for confirming the actual gastric resistance of tablets and powders. The machine is equipped with (i) a thermostat to maintain the temperature at 37 °C inside the stomach and intestine throughout the duration of the session and (ii) double digital-guided pumps capable of vacuuming FSSGF and FaSSIF at the right time according to preset software-based parameters (fasted or fed state). The machine simulates both the fasted and fed states by changing the frequency of contraction waves and the aspiration of different volumes of FSSGF and FaSSIF.

Considering RES-based LiBADDS tablets, LiBADDS phase absorption on solid tablet excipients may impair compressibility. In particular, the fatty phase reduces the hardness and increases the friability of tablets, thereby compromising their overall compatibility with production and blistering industrial processes. During the fabrication process, full solubilization of RES into the oily phase is a priority. RES is poorly soluble in most vegetal oils and glycerides, but it has good solubility in PS80, especially at high temperatures. Efficient micellization in the intestine is expected to occur if RES is well solubilized in the lipid-based auto-emulsifying phase. Indeed, this physical phenomenon promotes the active interaction of RES with matrix components. The four tablets that passed the quality control and industrial fabrication steps (RES LiBADDSs 013, 017 and 019, and RES LiBADDS 015 with some limitations) were tested in the presence and absence of pancreatin. Unlike RES-N_aC-based tablets, the association between the LiBADDS phase and NaC changed the disaggregation behavior. In fact, the increase in N_aC content in the LiBADDS-based tablets appeared to prolong the disaggregation time. Generally, the average disaggregation time was lower for LiBADDS-based tablets than for N_aC-based tablets, highlighting the role of the LiBADDS phase in accelerating disaggregation (Fig. 5A-C).

Disaggregation time of LiBADDS-containing tablets in the presence or absence of pancreatin. (D) RES LiBADDS 013 (pancreatin vs no pancreatin); (E) RES LiBADDS 017 (pancreatin vs no pancreatin); (F) RES LiBADDS 019 (pancreatin vs no pancreatin). (G) Disaggregation time of RES LiBADDS 013 vs RES LiBADDS 017 vs RES LiBADDS 019. (T-test, Anova, $p < 0.05$).

For RES-N_aC -based tablets, pancreatin plays a central role in fostering tablet disaggregation, confirming that N_aC works as a “modulating release matrix” (Fig. 5D-F). The shortest disaggregation time was measured with RES-based LiBADDS 019, which had the highest PS80/RES ratio and the lowest N_aC /(PS80/RES) ratio (Fig. 5G, Eq. (5)).

$$t_{disagg.} = N_aC/(PS80\,/\,RES) \tag{5}$$

where t_{disagg} is the tablet disaggregation time, N_aC is the sodium caseinate content of the tablet, PS80 is the polysorbate 80 content of the tablet, and RES is the resveratrol content of the tablet.

To further confirm these data, the largest difference in the disaggregation time between RES-N_aC-based and RES-based LiBADDS tablets containing the same N_aC content (101 min) was recorded for RES LiBADDS 019. On the basis of these data, a linear correlation could be established between the N_aC (PS80/RES) ratio and disaggregation time ($R^2 = 0{,}992$), suggesting a direct relationship between the PS80/RES ratio and disaggregation time and an inverse correlation between the N_aC and disaggregation time (Fig. 6).

Thus, the higher the PS80/RES ratio and the lower the N_aC content were, the faster the RES-based LiBADDS tablets disaggregated. This may be due to optimized solubilization of RES into the LiBADDS phase, which has a relatively high PS80/RES ratio. Therefore, it may be argued that the solubilization rate of RES into the LiBADDS phase is strictly related to the PS 80 content and is directly correlated with the disaggregation time. In contrast, RES-based tablets without N_aC completely disaggregated in FSSGF in 20 - 35 min.

3.3. RES-based LiBADDS tablet characterization

To assess whether RES physically interacted with the matrix, DSC analysis was performed. DSC is an analytical tool that identifies the physical properties and energy transitions of materials exposed to a constant heat flux in relation to temperature. This analytical tool is used to estimate the amorphous or crystalline structure of the analysed material in relation to enthalpy changes. It is also possible to identify the glass transition temperature (T_g), melting temperature (T_m) and crystallization temperature (T_c) by monitoring changes in heat absorption or

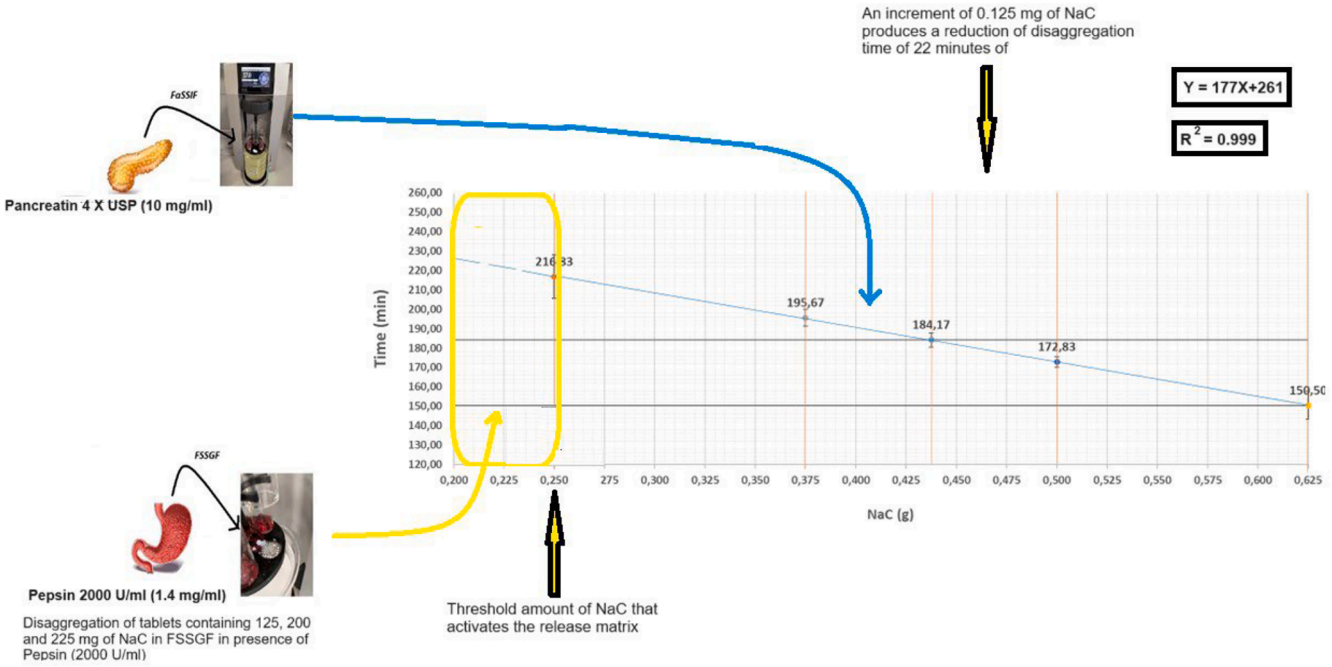

Fig. 3. Plot of the disaggregation time versus the N_aC content. In the range between 250 and 625 mg, the higher the content of N_aC was, the lower the disaggregation time of the tablets. This correlation is linear, with R^2=0,9998, and the corresponding line equation was calculated. However, this disaggregation behaviour fails between 125 and 225 mg N_aC, with tablets already disaggregated in FSSGF lacking gastric resistance (Anova, $p < 0.05$).

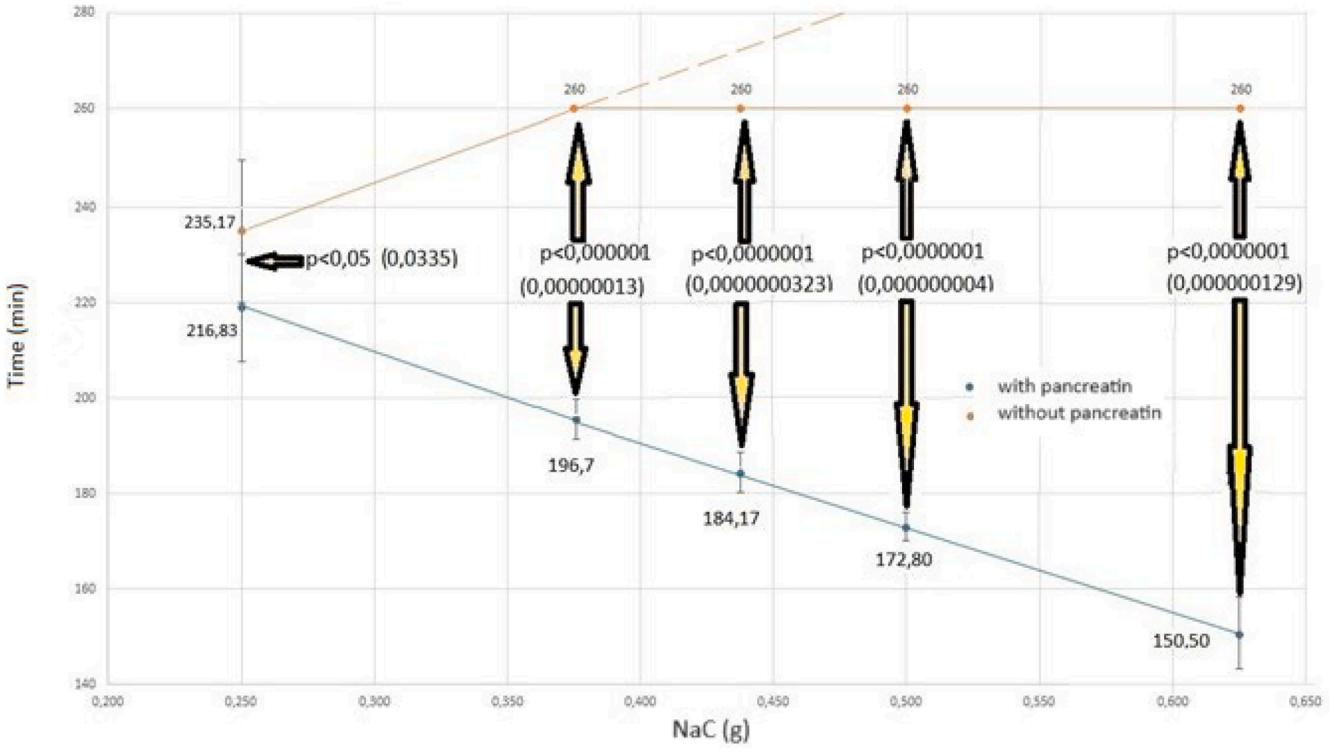

Fig. 4. Relationship between the N_aC content and disaggregation time in both FSSGF models in the presence or absence of pancreatin. In the presence of pancreatin, a clear linear inverse correlation between the N_aC content and disaggregation time was observed, whereas in the absence of pancreatin, the correlation between the N_aC content and disaggregation time appeared to be direct. Furthermore, in the absence of pancreatin, with the sole exception of 250 mg N_aC, the disaggregation time was greater than 260 min. (T-test, Anova $p < 0.05$).

release (endothermic or exothermic processes). Specifically, DSC can determine a structural shift from the crystalline to the amorphous state of an active ingredient entrapped into a composite matrix.

From the overlapping thermograms shown in Fig. 7A, an almost complete disappearance of the RES endothermic peak in the RES-based LiBADDS 019 tablet curve was clearly appreciable.

In the thermograms of the RES-based LiBADDS 013 and 017 tablets, the RES crystalline peaks also disappeared (thermograms are available

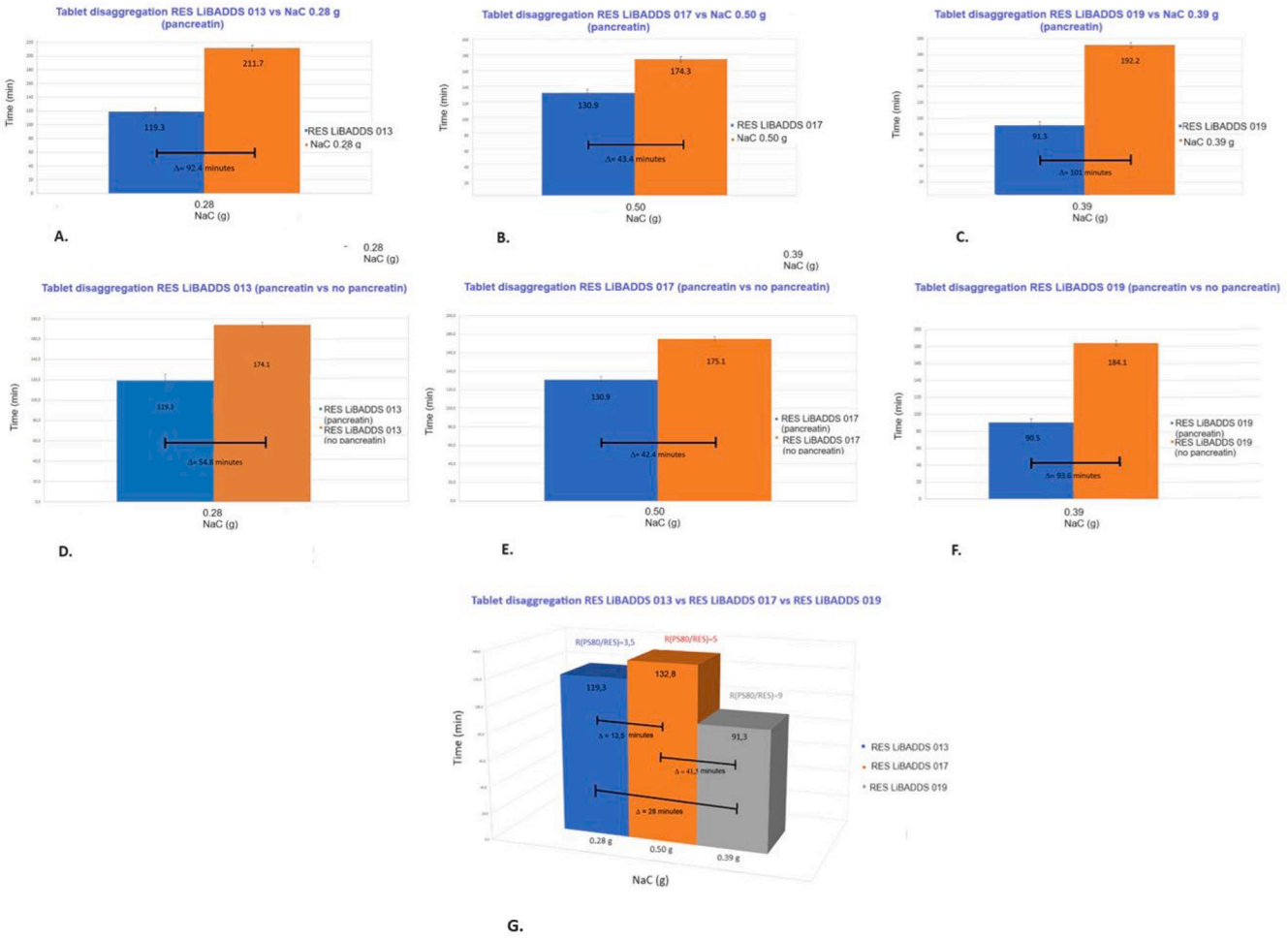

Fig. 5. Disaggregation time of N_aC-containing tablets vs. LiBADDS-containing tablets with the same N_aC content. (A) RES LiBADDS 013 vs 0.28 g N_aC; (B) RES LiBADDS 017 vs 0.50 g N_aC; (C) RES LiBADDS 019 vs 0.39 g N_aC.

in the Supplementary material Section, Fig. S1). In the DSC curve of the RES-based LiBADDS 019 tablet, only the endothermic peak attributable to pure GBD was visible. This is likely due to RES being molecularly dispersed in the melted mixture of GBD and PS80 in an amorphous form or to the fact that RES is forced to dissolve in the melted excipient mixture upon heating. The molecular interaction with the matrix is pivotal for changing the overall bioaccessibility of RES in the intestine through the generation of mixed micelles. This phenomenon was confirmed via X-ray diffraction analysis, as shown by a comparison of overlapping X-ray images (Fig. 7B).

RES showed characteristic peaks at 4.311, 6.687 (the most intense), 13.286, 16.416, 19.207, 25.316, and 28.144° of 2 theta. For the RES-based LiBADDS 019 tablet, a halo characteristic of an amorphous sample in the 2 theta range of 12–30° is evident, with the disappearance of the RES peaks, indicating that full RES solubilization into the LiBADDS matrix took place.

RES-based LiBADDS 013 and 017 tablet X-ray graphs (X Rays graphs are available in the Supplementary material Section, Fig. S2) revealed RES crystalline peaks, indicating that the apparent RES amorphization suggested by DSC thermograms is most likely due to “forced” solubilization of RES into the LiBADDS matrix because of the energy supply. This is also consistent with the much higher PS80/RES ratio for RES-based LiBADDS 019 than for RES-based LiBADDSs 013 and 017 (Table 1). These results provide further evidence that RES needs to be solubilized into PS80 to yield effective encapsulation in the LiBADDS matrix.

Finally, size analysis of RES-based LiBADDS 019 dispersed in FaSSIF was performed via DLS. The results indicated the presence of nano-dimensioned micelles with an average diameter of 190 nm and a polydispersity index (PDI) of 0.188 (Supplementary materials Section, Fig. S4; Table 4).

Notably, dispersion occurred in FaSSIF at 37 °C in the presence of pancreatin, suggesting that the formation of nanosized mixed micelles was spontaneous at physiologic temperature and did not require a large amount of energy load to be generated. This phenomenon is due to the presence of several different active surfacing agents, such as PS 80, GDB, N_aC, CLA, and bile salts. CLA becomes an active surface agent above pH 6 since it occurs in its carboxylic form. From the size analysis, it may be inferred that RES-based LiBADDS 019 generated a fine micellar dispersion with a low PDI. These data support the crucial role of RES solubilization in the LiBADDS phase (PS80/RES ratio) to produce fine micellar dispersion and dimensional uniformity. The z potential is low despite the presence of both N_aC and CLA, which are negatively charged at pseudo-neutral intestinal pH.

3.4. Assessment of bioaccessible fraction RES-based tablets and RES-based LiBADDS tablets

Table 5 shows the RES bioaccessibility percentage registered after simulated gastrointestinal digestion for RES-based LiBADDSs 013, 015, 017, and 019 and for unformulated RESs (RES-based tablets). The obtained values indicated that RES was usefully entrapped within the micelles that represent the bioaccessible fraction. In contrast, the RES found in pellets, i.e., the nonbioaccessible fraction, was very low. RES-

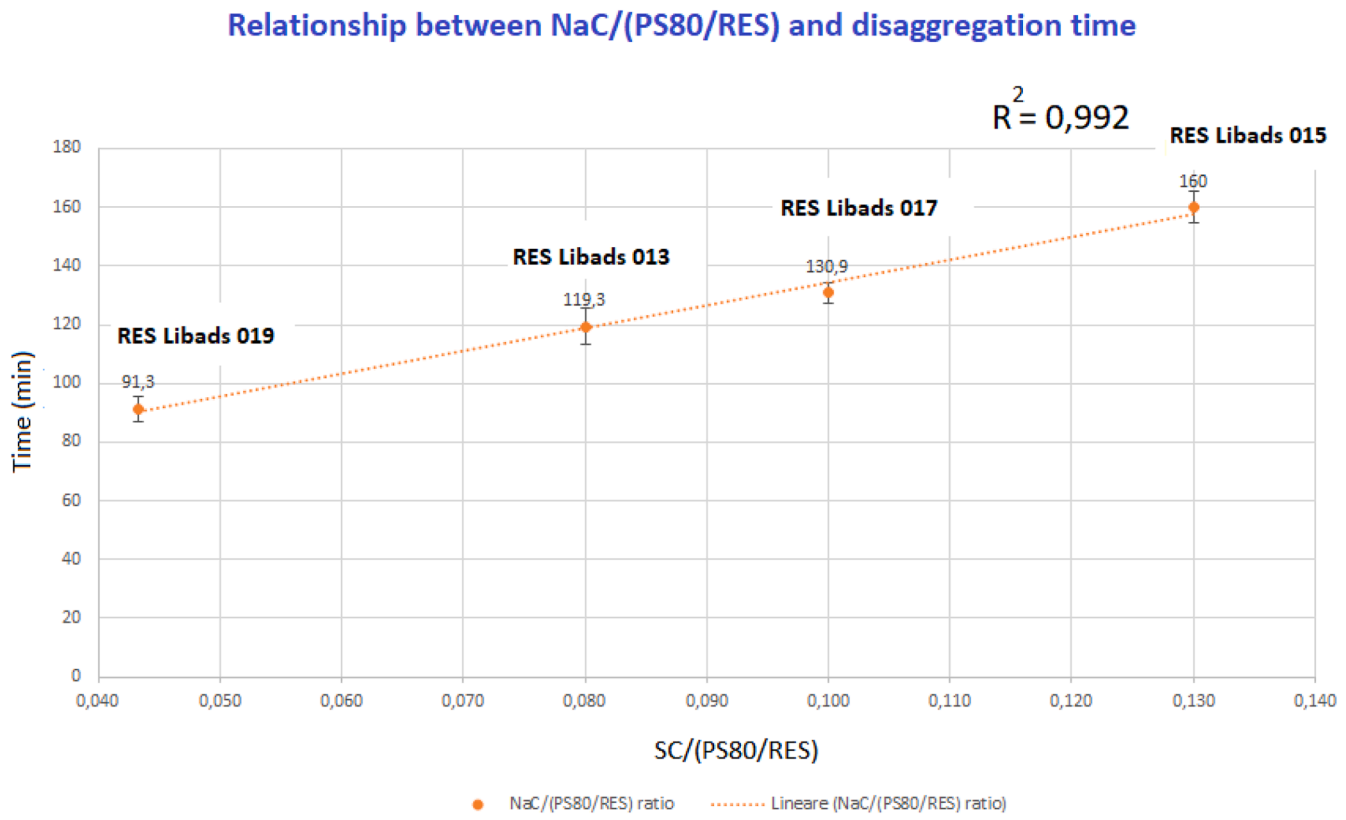

Fig. 6. Graph showing the disaggregation time of LiBADDS-containing tablets against the N_aC/(PS80/RES) ratio. A pseudolinear correlation with R^2=0,992 appears, suggesting a direct relationship between the PS80/RES ratio and disaggregation time and an inverse relationship between N_aC and the disaggregation time. (Anova, $p < 0.05$).

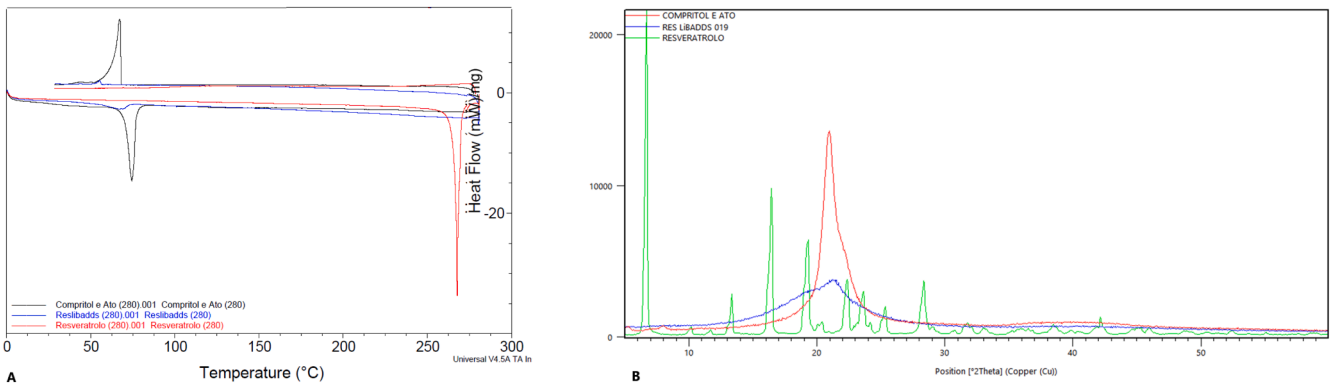

Fig. 7. (A) Overlapping DSC of RES LiBADDS 019, Compritol and RES. (B) Overlapping X-ray diffraction of RES LiBADDS 019, Compritol and RES.

Table 4
Average size of mixed micelles of RES-based LiBADDS 019 dispersed in FaSSIF. PDI polydispersity index.

Sample	Filtered 0.450 mm
Temperature	25 °C
Z-average	157 (±23) nm
Intensity Mean (diameter) peak	192 (±) nm
PdI	0.188 (±0.004)
Attenuator	5
Mean Count Rate (DLS)	139 (±) kcps
Measurement Position (mm)	4.65
Zeta potential	−14 (±2) mV

based LiBADDS 019 had a very high BF% (94 %), whereas unformulated RES had the highest value (98.7 %), with no pellet collected after centrifugation, which is consistent with very high RES bioaccessibility at the intestinal level, as described by Walle et Maier/Salamon (Walle, 2011; Maier-Salamon et al., 2006). Thus, the higher the PS80/RES ratio is, the greater the BF, which is in accordance with the hypothesis that RES solubilization represents a crucial factor for increasing bioaccessibility. Taken together, these data support the hypothesis that RES-based LiBADDSs represent a valid technological tool for delivering RES in a highly bioaccessible form.

The next step of this research was to investigate the RES release kinetics and mechanism from RES-based LiBADDS tablets. Fig. 8A shows the pseudolinear trend (R^2 = 0,984) of the RES delivery rate, suggesting a kinetic model of delivery close to the zero-order model with a minimal initial burst (Table 6).

Table 5
RES bioaccessibility (BF%) of six RES-based LiBADDSs: 013, 015, 017, and 019 tablets and six RES-based tablets. RES was quantified as *cis*+trans isomers. (Anova, $p < 0.05$).

Formulation	RES in pellett (mg)	RES in supernatant (mg)	RES total recovery (mg)	RES theoretical (mg)	Bioaccessibility (BF) (%)
RES-based LiBADDS 013	1.76±0.14	36.55±3.80	49.8 ± 3.60	60	73.4
RES-based LiBADS 015	6.40±0.52	43.6 ± 4.60	54.9 ± 5.80	60	79.4
RES-based LiBADS 017	4.80±0.26	44.4 ± 3.50	51.0 ± 6.80	60	87.0
RES-based LiBADS 019	1.20±0.19	24.8 ± 1.80	26.4 ± 3.90	30	94.0
RES-based	0	29,6 ± 1.40	29.6 ± 3.90	30	98.7

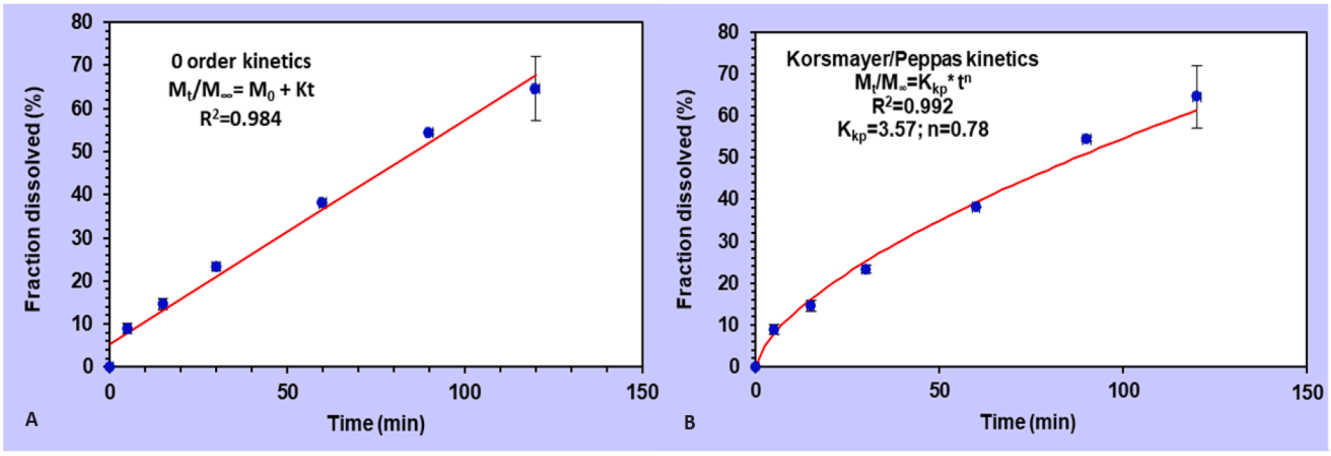

Fig. 8. (A). Fitting of the release kinetics of RES from RES LiBADDS 019 with a 0-order kinetic model (R^2=0,984). (B) Fitting of the release kinetics of RES from RES LiBADDS 019 with the Korsmayer/Peppas kinetics model (R^2=0,992).

Table 6
Main parameters of the RES-based LiBADDS 019 tablet disaggregation graph according to the zero-order and Korsmayer/Peppas kinetic models.

	Zero-order kinetics	Korsmayer/Peppas kinetics
Equation	$M_t/M_\infty = M_0 + Kt$	$M_t/M_\infty = K_{kp} * t^n$
R^2	0.984	0.992
K	0,52	–
K_{kp}	–	3.57
n	–	0.78

To determine the real mechanism of RES release from the LiBADDS matrix, first, 60 % of the release curve was fitted with the Korsmeyer–Peppas model (6) (Korsmeyer and Peppas, 1984; Peppas and Sahlin, 1989), which substantially indicates a non-Fickian drug transport mechanism of delivery (R^2 = 0.992) (Fig. 8B) and a prevalent erosion drug release mechanism.

$$M_t/M_\infty = K_{kp} * t_n \quad (6)$$

where Mt is the fractional drug release at time t, M_∞ is the amount of drug loading at infinite time, K_{kp} is the Korsmayer–Peppas constant, which considers the structural and geometric characteristics of the delivery system, and n is the parameter describing the mechanism of transport of the drug through the matrix.

These data suggest that LiBADDS technology promotes constant RES delivery over time through slow tablet imbibition and erosion processes into the FaSSIF medium. The N_aC-based matrix is thought to be gradually hydrolysed by proteolytic enzymes of pancreatin, leading to sustained, concentration-independent RES release. This pattern seems to be consistent with the "slow-release matrix" features postulated for LiBADDS technology. Interestingly, the overall complete dissolution time for RES-based LiBADDS 019 was greater than 240 min, whereas the overall disaggregation time was 90 min. Once again, this highlights the substantial difference between these two tests in predicting the delivery of a poorly soluble drug from a solid form, according to the Europeam Pharmacopeia and ICH guidelines (Radwan et al., 2014; Nickerson et al., 2018). The RES-based LiBADDS tablets presented unique features of a matrix composed of a hydrosoluble polymer that was slowly degraded and eroded through solubilization and cleavage of N_aC by proteolytic enzymes. N_aC solubilization most likely increases upon hydrolysis. Another key feature driving the dissolution rate is the presence of different surfactants that work as "water attracting agents". Among others, PS80 plays a crucial role in both accelerating disaggregation and solubilizing RES.

3.5. Cells viability

The cytotoxicity assessment suggested that there is no toxic effect of undiluted RES LiBADDS 019 BF in FaSSIF on the monolayer (Supplementary material, Table S2).

3.6. RES permeation

After verifying the absence of toxicity for both unformulated RES and RES-based LiBADDS 019 on Caco-2 cells, RES permeation was investigated. The TEER values of the monolayer before the addition of the RES-based formulations were greater than 500 Ohm/cm^2, reflecting the firmness and integrity of the monolayer. Further determination of LY passage through the monolayer after 1 h revealed fluorescence values close to 0 and P_{app} (cm/s) values lower than 5×10^8, which confirmed the substantial integrity of the Caco-2 tight junctions. After 1, 2, and 3 h since the application of RES-based LiBADDS 019 after digestion at its maximal nontoxic concentration at the apical side, the TEER values indicated no changes in monolayer integrity (TEER values are reported in the Supplementary materials Section, Table S1). In contrast, on the basolateral side, significant changes (25–30 % reduction) in TEER values were observed; however, the TEER values were far greater than the lower threshold value accepted in the range of 200–250 Ohm/cm^2 to define monolayer integrity (Karakocak et al., 2023). Similar

considerations were speculated for unformulated RES. The difference in terms of the reduction in TEER between the RES LiBADDS formulation and unformulated RES at 1, 2, 3, and 24 h was inconsistent, indicating that the RES LiBADDS formulation did not significantly affect monolayer integrity (TEER values). The P_{app} (cm/s) values of LY calculated after the application of RES LiBADDS 019 and unformulated RES at 3 h are very close to those at time 0, confirming that the LiBADDS formulation did not affect the integrity of the tight junctions in the monolayer.

The results obtained from the permeation assays indicated that a nonlinear model fitted the permeation curve for both A-B and B-A passages, suggesting a high absorption profile of RES from RES-based LiBADDS 019 (Fig. 9A and B, Table 7). In this case, the non-sink model Artursson's Eq. (2) was applied to calculate P_{app}. With respect to the unformulated RES, a linear model was fitted with permeation for both the A-BL and BL-A passages (Fig. 9C and D, Table 7). In this case, the sink model Eq. (1) was applied to calculate P_{app}.

The calculated P_{app} value for RES-based LiBADDS 019 was significantly greater than that registered for unformulated RES (Table 6), indicating the significant role of LiBADDS technology in enhancing the RES permeation profile.

The P_{app} (B-A)/P_{app} (A-B) ratio calculated for RES-based LiBADDS 019 indicated that the efflux ratio (ER) was much lower than 1, suggesting negligible efflux activity mediated by P-gp and other ABC transporters. Interestingly, this ER value was lower than that of unformulated RES, which, in turn, was in accordance with the literature data (Vasconcelos et al., 2019; Li et al., 2003).

This suggests an active role of the LiBADDS formulation and, more likely, of PS80 in reducing P-gp- and ABC-mediated active extrusion, as reported in the literature (Rathod et al., 2022; Moesgaard et al., 2022). The data related to the unformulated RES P_{app} are in accordance with those reported by Neves for RES at similar concentrations digested in FaSSIF (Neves et al., 2016). The mass balances for RES-based LiBADDS 019 and unformulated RES were approximately 75 % and 80 %, respectively, for both absorption directions.

Table 7
P_{app}, % permeation and mass balance of RES from RES LiBADS 019 and unformulated RES in both the A-B and B-A directions after 3 h. The results are expressed as the means of 3 independent experiments ± SDs carried out in duplicate. (T-test, $p < 0.05$).

RES LiBADDS (A B) C = 5.51 μm	RES LiBADDS (B A) C = 5.51 μm
P_{app} 1.24×10^-4 ± 1.63×10^−5 % permeation (A-B) (3 h) 48.8 ± 3.62 mass balance 75.9 ± 11.3	P_{app} 7.12×10^-5 ± 8.64×10^−6 %permeation (A-B) (3 h) 24.5 ± 3.04 mass balance 75.0 ± 8.44
Unformulated RES (A B) C = 6.13 μm	Unformulated RES (B A) C = 6.13 μm
P_{app} 3.02×10^-5 ± 3.68×10^−6 %permeation (A-B) (3 h) 24.1 ± 2.38 mass balance 83.8 ± 8.29	P_{app} 2.83×10^-5 ± 3.59×10^−6 %permeation (A-B) (3 h) 15.1 ± 2.38 mass balance 75.6 ± 9.03

The RES permeability of unformulated RES and RES-based LiBADDS 019 was calculated considering the RES fraction present in the supernatant bulk after simulated digestion. In fact, the supernatant fraction represents the BF of RES that can fully permeate through the intestinal epithelium, preventing its absorption. On the other hand, the so-called "pellet" non-dispersible RES fraction resulting from centrifugation of the digested dispersion represents the insoluble fraction that cannot permeate through the intestine. For this reason, it was not tested with the Caco-2 cell intestinal monolayer. Approximately 48 % (48.8 ± 3.62 %) of the initial RES dose present in RES-based LiBADDS permeated from the apical to basolateral side, unlike the unformulated RES, for which only 24.1 ± 2.38 % of the initial dose permeated. Therefore,

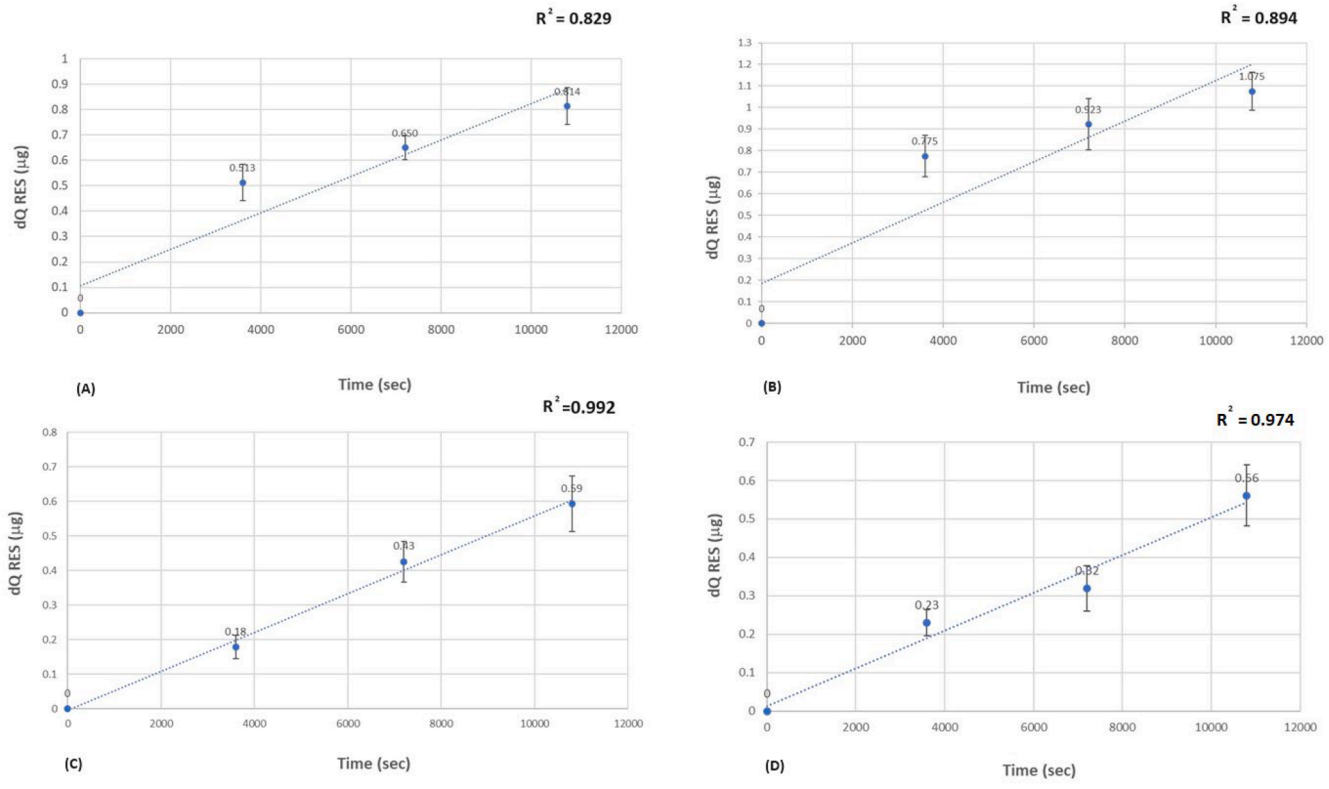

Fig. 9. (A) Graph showing the permeated RES (dQ μg) against time (*sec*) from RES LiBADDS 019 in the apical to basolateral direction. The curve describes a nonlinear trend, suggesting a nonlinear fitting model of permeation. (B) Graph showing the permeated RES (dQ μg) against time (*sec*) from RES LiBADDS 019 in the basolateral to the apical direction. The curve describes a nonlinear trend, suggesting a nonlinear fitting model of permeation. (C) Graph showing the permeated RES (dQ μg) against time (*sec*) from the unformulated RES in the apical to the basolateral direction. The curve describes a pseudolinear trend model of permeation. (D) Graph showing the permeated RES (dQ μg) against time (*sec*) from the unformulated RES in the basolateral to the apical direction. The curve describes a pseudolinear trend model of permeation. (T-test, $p < 0.05$).

LiBADDS technology significantly increased RES monolayer permeation in the A-B directions, as suggested by the permeation rates and P_{app} values, which were approximately 2-fold and 4-fold greater than those of unformulated RES, respectively. The mass recovery rate was greater than 75 % for both the A-B and B-A directions.

4. Conclusions

The formulation of lipid-based auto-emulsifying drug delivery systems (LIBADDSs) has garnered attention for enhancing the delivery of small lipophilic molecules in bioaccessible forms within the intestine. This study introduces a novel LIBADDS in tablet form designed to deliver RES encapsulated in nanosized micelles to the small intestine, aiming to improve RES intestinal permeability in unmodified form. The key technological concept driving this LIBADDS design involves combining N_aC, PS80, and CLA at precise ratios to promote tablet disaggregation in the small intestine and increasing RES permeability by likely reducing intestinal presystemic metabolism and affecting efflux transport rate.

This work provides the first evidence that N_aC acts effectively as a gastric resistance agent, with tablets passing gastric resistance tests across a wide range of N_aC concentrations, even in the presence of pepsin. Disaggregation experiments in FaSSIF revealed a linear correlation between the N_aC content and tablet disaggregation time, highlighting the potential of N_aC as both a reliable enteric coating and modulator of sustained intestinal release.

The RES-N_aC-LiBADDS tablets were shown to release RES in the intestine according to the N_aC /(PS80/RES) ratio, with RES release activated by pancreatin following pseudolinear non-Fickian kinetics predominantly through an erosion mechanism. The molecular interactions between RES and the lipid-surfactant matrix of LiBADDS were confirmed through DSC and PXRD analyses.

Permeability studies across Caco-2 monolayers demonstrated a two-fold increase in RES permeation from LIBADDS compared with unformulated RES, with a fourfold increase in the permeability coefficient (P_{app}). Despite the similar bioaccessibility (BF) between LIBADDSs and unformulated RESs, the enhanced permeation is attributed to LIBADDS technology, which is likely facilitated by excipients such as PS80, which may reduce RES presystemic metabolism and affecting extrusion process, as previously reported.

Experimental findings suggest that LIBADDS formulation containing PS80, may impair ABC transporter activity, reducing RES efflux from the basolateral chambers to the apical chambers. This is supported by a significant reduction in the RES efflux ratio (ER) compared with that of unformulated RES, indicating a role of LIBADDS in modulating intestinal cell function.

Overall, these results support the potential of N_aC-based LIBADDSs in enhancing RES intestinal permeability in its unmodified form and reducing extrusion process of RES mediated by ATP-binding cassettes. A clinical trial, particularly phase 1 pharmacokinetic study with a crossover design in human volunteers, is warranted to confirm whether this technology effectively improves the bioavailability of RES compared to the non-formulated one.

Ethical statement

Ethics approval and consent to participate n.t.d.

Consent for publication

All the authors mentioned in this paper allow publication.

Data availability

The data that support the findings of this study are available upon request from the corresponding author, [AF]. The data are not publicly available because they contain sensible information about a filed patent not yet published.

Funding

No funding was received.

CRediT authorship contribution statement

Andrea Fratter: Writing – original draft, Validation, Supervision, Methodology, Investigation. **Andrea Cignarella:** Writing – review & editing, Validation, Supervision, Methodology. **Giovanni Eugenio Ramaschi:** Validation, Investigation. **Adele Papetti:** Writing – review & editing, Validation, Supervision, Methodology. **Vanessa Pellicorio:** Methodology, Investigation, Data curation. **Chiara Milanese:** Writing – review & editing, Supervision, Methodology. **Luca Casettari:** Writing – original draft, Validation. **Chiara Bolego:** Writing – original draft, Validation, Supervision, Methodology, Investigation.

Declaration of competing interest

The authors have no conflicts of interest to declare.

Acknowledgments

Our thanks go to Laboratorio della Farmacia SpA, Quarto d'Altino, Venice, for their valuable support in carrying out the formulative activities and raw material supply chain.

Supplementary materials

Supplementary material associated with this article can be found, in the online version, at doi:10.1016/j.ejps.2024.106912.

References

Acharya, D.P., Sanguansri, L., Augustin, M.A., 2013a. Binding of resveratrol with sodium caseinate in aqueous solutions. Food Chem. 141 (2), 1050–1054. https://doi.org/10.1016/j.foodchem.2013.03.037.

Acharya, D.P., Sanguansri, L., Augustin, M.A., 2013b. Binding of resveratrol with sodium caseinate in aqueous solutions. Food Chem. 141 (2), 1050–1054. https://doi.org/10.1016/j.foodchem.2013.03.037. Nov 15.

Acta Pharmaceutica Sinica. Volume 11, Issue 8, 2021, Pages 2449–2468, 10.1016/j.apsb.2020.12.022.

Amri, A., Chaumeil, J.C., Sfar, S., Charrueau, C., 2012a. Administration of resveratrol: what formulation solutions to bioavailability limitations? J. Control Release 158 (2), 182–193. https://doi.org/10.1016/j.jconrel.2011.09.083. Mar 10.

Amri, A., Chaumeil, J.C., Sfar, S., Charrueau, C., 2012b. Administration of resveratrol: what formulation solutions to bioavailability limitations? J. Control Release 158 (2), 182–193. https://doi.org/10.1016/j.jconrel.2011.09.083.

Artursson, P., Palm, K., Luthman, K., 2001. Caco-2 monolayers in experimental and theoretical predictions of drug transport. Adv. Drug Deliv. Rev. 46 (1–3), 27–43. https://doi.org/10.1016/s0169-409x(00)00128-9. Mar 1.

Bailey, H.H., Johnson, J.J., Lozar, T., Scarlett, C.O., Wollmer, B.W., Kim, K., Havinghurst, T., Ahmad, N., 2021. A randomized, double-blind, dose-ranging, pilot trial of piperine with resveratrol on the effects on serum levels of resveratrol. Eur. J. Cancer Prev. 30 (3), 285–290. https://doi.org/10.1097/CEJ.0000000000000621.

Bertelli, A.A., Das, D.K., 2009. Grapes, wines, resveratrol, and heart health. J. Cardiovasc. Pharmacol. 54 (6), 468–476. https://doi.org/10.1097/FJC.0b013e3181bfaff3. Dec.

Brodkorb, A., Egger, L., Alminger, M., Alvito, P., Assunção, R., Ballance, S., Bohn, T., Bourlieu-Lacanal, C., Boutrou, R., Carrière, F., Clemente, A., Corredig, M., DuPont, D., Dufour, C., Edwards, C., Golding, M., Karakaya, S., Kirkhus, B., Le Feunteun, S., Lesmes, U., Macierzanka, A., Mackie, A.R., Martins, C., Marze, S., McClements, D.J., Ménard, O., Minekus, M., Portmann, R., Santos, C.N., Souchon, I., Singh, R.P., Vegarud, G.E., Wickham, M.S.J., Weitschies, W., Recio, I., 2019. INFOGEST static in vitro simulation of gastrointestinal food digestion. Nat. Protoc. 14 (4), 991–1014. https://doi.org/10.1038/s41596-018-0119-1. Apr.

Bu, P., Ji, Y., Narayanan, S., Dalrymple, D., Cheng, X., Serajuddin, A.T., 2017. Assessment of cell viability and permeation enhancement in presence of lipid-based self-emulsifying drug delivery systems using Caco-2 cell model: polysorbate 80 as the surfactant. Eur. J. Pharm. Sci. 99, 350–360. https://doi.org/10.1016/j.ejps.2016.12.018. Mar 1.

Cerpnjak, K., Zvonar, A., Gašperlin, M., Vrečer, F., 2013. Lipid-based systems as a promising approach for enhancing the bioavailability of poorly water-soluble drugs. Acta Pharm. 63 (4), 427–445. https://doi.org/10.2478/acph-2013-0040. Dec.

Di Prima, G., Angellotti, G., Scarpaci, A.G., Murgia, D., D'agostino, F., Campisi, G., De Caro, V., 2021. Improvement of resveratrol permeation through sublingual mucosa: chemical permeation enhancers versus spray drying technique to obtain fast-disintegrating sublingual mini-tablets. Pharmaceutics. 13 (9), 1370. https://doi.org/10.3390/pharmaceutics13091370. Aug 31.

European Pharmacopoeia, 6.2, European Treaty Series, Council of Europe ISSN 0070-105X. 2024.

Francioso, A., Mastromarino, P., Masci, A., d'Erme, M., Mosca, L., 2014. Chemistry, stability and bioavailability of resveratrol. Med. Chem. 10 (3), 237–245. https://doi.org/10.2174/1573406411309660053. May.

Geboers, S., Stappaerts, J., Tack, J., Annaert, P., Augustijns, P., 2016. In vitro and in vivo investigation of the gastrointestinal behavior of simvastatin. Int. J. Pharm. 510 (1), 296–303. https://doi.org/10.1016/j.ijpharm.2016.06.048. Aug 20.

Gertz, M., Nguyen, G.T., Fischer, F., Suenkel, B., Schlicker, C., Fränzel, B., Tomaschewski, J., Aladini, F., Becker, C., Wolters, D., Steegborn, C., 2012. A molecular mechanism for direct sirtuin activation by resveratrol. PLoS One 7 (11), e49761. https://doi.org/10.1371/journal.pone.0049761.

Hubatsch, I., Ragnarsson, E.G., Artursson, P., 2007. Determination of drug permeability and prediction of drug absorption in Caco-2 monolayers. Nat. Protoc. 2 (9), 2111–2119. https://doi.org/10.1038/nprot.2007.303.

Hung, Li-M, Chen, J.-K., Huang, S.-S., Lee, R.-S., Su, M.-J., 2000. Cardioprotective effect of resveratrol, a natural antioxidant derived from grapes. Cardiovasc. Res. 47 (3), 549–555. https://doi.org/10.1016/S0008-6363(00)00102-4. August.

Johnson, J.J., Nihal, M., Siddiqui, I.A., Scarlett, C.O., Bailey, H.H., Mukhtar, H., Ahmad, N., 2011. Enhancing the bioavailability of resveratrol by combining it with piperine. Mol. Nutr. Food Res. 55 (8), 1169–1176. https://doi.org/10.1002/mnfr.201100117.

Karakocak, B.B., Keshavan, S., Gunasingam, G., Angeloni, S., Auderset, A., Petri-Fink, A., Rothen-Rutishauser, B., 2023. Rethinking of TEER measurement reporting for epithelial cells grown on permeable inserts. Eur. J. Pharm. Sci. 188, 106511. https://doi.org/10.1016/j.ejps.2023.106511. Sep 1.

Korsmeyer, R.W., Peppas, N.A., 1984. Solute and penetrant diffusion in swellable polymers. III. Drug release from glassy poly(HEMA-co-NVP) copolymers. J. Cont. rel. 1 (2), 89–98. https://doi.org/10.1016/0168-3659(84)90001-4.

Li, Y., Shin, Y.G., Yu, C., Kosmeder, J.W., Hirschelman, W.H., Pezzuto, J.M., van Breemen, R.B., 2003. Increasing the throughput and productivity of Caco-2 cell permeability assays using liquid chromatography–mass spectrometry: application to resveratrol absorption and metabolism. Comb. Chem. High. Throughput. Screen. 6 (8), 757–767. https://doi.org/10.2174/138620703771826865. Dec.

Madan, J.R., Ansari, I.N., Dua, K., Awasthi, R., 2020. Formulation and in vitro evaluation of casein nanoparticles as carrier for Celecoxib. Adv. Pharm. Bull. 10 (3), 408–417. https://doi.org/10.34172/apb.2020.049. Jul.

Maier-Salamon, A., Hagenauer, B., Wirth, M., Gabor, F., Szekeres, T., Jäger, W., 2006. Increased transport of resveratrol across monolayers of the human intestinal Caco-2 cells is mediated by inhibition and saturation of metabolites. Pharm. Res. 23 (9), 2107–2115. https://doi.org/10.1007/s11095-006-9060-z. Sep.

Miki, H., Uehara, N., Kimura, A., Sasaki, T., Yuri, T., Yoshizawa, K., Tsubura, A., 2012. Resveratrol induces apoptosis via ROS-triggered autophagy in human colon cancer cells. Int. J. Oncol. 40 (4), 1020–1028. https://doi.org/10.3892/ijo.2012.1325. Apr.

Moesgaard, L., Reinholdt, P., Nielsen, C.U., Kongsted, J., 2022. Mechanism behind polysorbates' inhibitory effect on P-Glycoprotein. Mol. Pharm. 19 (7), 2248–2253. https://doi.org/10.1021/acs.molpharmaceut.2c00074. Jul 4.

Mudie, D.M., Murray, K., Hoad, C.L., et al., 2014. Quantification of gastrointestinal liquid volumes and distribution following a 240 mL dose of water in the fasted state. Mol. Pharm. 11, 3039–3047. https://doi.org/10.1021/mp500210c.

Neves, A.R., Martins, S., Segundo, M.A., Reis, S., 2016. Nanoscale delivery of resveratrol towards enhancement of supplements and nutraceuticals. Nutrients 8 (3), 131. https://doi.org/10.3390/nu8030131. Mar 2.

Nickerson, B., Kong, A., Gerst, P., Kao, S., 2018. Correlation of dissolution and disintegration results for an immediate-release tablet. J.Pharm. Biomed. Anal. 150, 333–340. https://doi.org/10.1016/j.jpba.2017.12.017.

Pandey, V., Kohli, S., 2018. Lipids and surfactants: the inside story of lipid-based drug delivery systems. Crit. Rev. Ther. Drug Carrier Syst. 35 (2), 99–155. https://doi.org/10.1615/CritRevTherDrugCarrierSyst.2018016710.

Peppas, N.A., Sahlin, J.J., 1989. A simple equation for the description of solute release. III. Coupling of diffusion and relaxation. Int. J. Pharm. 57, 169–172. https://doi.org/10.1016/0378-5173(89)90306-2.

Radwan, A., Wagner, M., Amidon, G.L., Langguth, P., 2014. Biopredictive tablet disintegration: effect of water diffusivity, fluid flow, food composition and test conditions. Eur. J. Pharm. Sci. 57, 273–279. https://doi.org/10.1016/j.ejps.2013.08.03833.

Rani, E.R., Radha, G.V., 2021. Insights into novel excipients of self-emulsifying drug delivery systems and their significance: an updated review. Crit. Rev. Ther. Drug Carrier Syst. 38 (2), 27–74. https://doi.org/10.1615/CritRevTherDrugCarrierSyst.2020034975.

Rathod, S., Desai, H., Patil, R., Sarolia, J., 2022. Nonionic surfactants as a P-glycoprotein (P-gp) efflux inhibitor for optimal drug delivery - a concise outlook. AAPS. PharmSciTech. 23 (1), 55. https://doi.org/10.1208/s12249-022-02211-1. Jan 18.

Salawi, A., 2022. Self-emulsifying drug delivery systems: a novel approach to deliver drugs. Drug Deliv. 29 (1), 1811–1823. https://doi.org/10.1080/10717544.2022.2083724. Dec.

Salla, M., Karaki, N., El Kaderi, B., Ayoub, A.J., Younes, S., Abou Chahla, M.N., Baksh, S., El Khatib, S., 2024. Enhancing the bioavailability of resveratrol: combine it, derivatize it, or encapsulate it? Pharmaceutics 16, 569. https://doi.org/10.3390/pharmaceutics16040569.

Sangsen, Y., et al., 2016. Influence of surfactants in self-microemulsifying formulations on enhancing oral bioavailability of oxyresveratrol: studies in Caco-2 cells and in vivo. Int. J. Pharm. 498 (1–2), 294–303. https://doi.org/10.1016/j.ijpharm.2015.12.002.

Schreck, K., Melzig, M.F., 2018. Intestinal saturated long-chain fatty acid, glucose and fructose transporters and their inhibition by natural plant extracts in Caco-2 cells. Molecules 23 (10), 2544. https://doi.org/10.3390/molecules23102544.

Sessa, M., Balestrieri, M.L., Ferrari, G., Servillo, L., Castaldo, D., D'Onofrio, N., Donsì, F., Tsao, R., 2014. Bioavailability of encapsulated resveratrol into nanoemulsion-based delivery systems. Food Chem. 147, 42–50. https://doi.org/10.1016/j.foodchem.2013.09.088. Mar 15.

Smoliga, J.M., Blanchard, O., 2014. Enhancing the delivery of resveratrol in humans: if low bioavailability is the problem, what is the solution? Molecules. 19, 17154–17172. https://doi.org/10.3390/molecules191117154.

Tavelin, S., Gråsjö, J., Taipalensuu, J., Ocklind, G., Artursson, P., 2002. Applications of epithelial cell culture in studies of drug transport. Methods Mol. Biol. 188, 233–272. https://doi.org/10.1385/1-59259-185-X:233.

Thaung Zaw, J.J., Howe, P.R., Wong, R.H, 2021. Long-term effects of resveratrol on cognition, cerebrovascular function and cardio-metabolic markers in postmenopausal women: a 24-month randomized, double-blind, placebo-controlled, crossover study. Clin. Nutr. 40 (3), 820–829. https://doi.org/10.1097/FJC.0b013e3181bfaff3. Mar.

Trevaskis, N.L., Charman, W.N., Porter, C.J., 2008. Lipid-based delivery systems and intestinal lymphatic drug transport: a mechanistic update. Adv. Drug Deliv. Rev. 60 (6), 702–716. https://doi.org/10.1016/j.addr.2007.09.007. Mar 17.

Van Slyke, L.L., Bosworth, A.W., 1913. Valency of molecules and molecular weights of casein and paracasein. J. Biol. Chem. 14, 227–230. https://doi.org/10.1016/S0021-9258(18)88593-3.

Vasconcelos, T., Araújo, F., Lopes, C., Loureiro, A., das Neves, J., Marques, S., Sarmento, B., 2019. Multicomponent self-nano emulsifying delivery systems of resveratrol with enhanced pharmacokinetics profile. Eur. J. Pharm. Sci. 137, 105011. https://doi.org/10.1016/j.ejps.2019.105011. Sep 1.

Vesely, O., Baldovska, S., Kolesarova, A., 2021. Enhancing bioavailability of nutraceutically used resveratrol and other stilbenoids. Nutrients 13 (9), 3095. https://doi.org/10.3390/nu13093095. Sep 2PMID: 34578972.

Vitaglione, P., Sforza, S., Galaverna, G., Ghidini, C., Caporaso, N., Vescovi, P.P., Fogliano, V., Marchelli, R., 2005. Bioavailability of trans-resveratrol from red wine in humans. Mol. Nutr. Food Res. 49 (5), 495–504. https://doi.org/10.1002/mnfr.200500002. May.

Vrbanac, H., Trontelj, J., Berglez, S., Petek, B., Opara, J., Jereb, R., Krajcar, D., Legen, I., 2020. The biorelevant simulation of gastric emptying and its impact on model drug dissolution and absorption kinetics. Eur. J. Pharm. Biopharm. 149, 113–120. https://doi.org/10.1016/j.ejpb.2020.02.002. Apr.

Walle, T., Hsieh, F., DeLegge, M.H., Oatis Jr, J.E., Walle, U.K., 2004. High absorption but very low bioavailability of oral resveratrol in humans. Drug Metab. Dispos. 32 (12), 1377–1382. https://doi.org/10.1124/dmd.104.000885. Dec.

Walle, T., 2011. Bioavailability of resveratrol. Ann. N. Y. Acad. Sci. 1215, 9–15. https://doi.org/10.1111/j.1749-6632.2010.05842.x.

Wang, X., Ye, A., Lin, Q., Han, J., Singh, H., 2018. Gastric digestion of milk protein ingredients: study using an in vitro dynamic model. J. Dairy. Sci. 101 (8), 6842–6852. https://doi.org/10.3168/jds.2017-14284. Aug.

Wong, R.H., Thaung Zaw, J.J., Xian, C.J., Howe, P.R, 2020. Regular supplementation with resveratrol improves bone mineral density in postmenopausal women: a randomized, placebo-controlled trial. J. Bone Miner. Res. 35 (11), 2121–2131. https://doi.org/10.1097/FJC.0b013e3181bfaff3. Nov.

Wu, J.M., Hsieh, T.C., 2011. Resveratrol: a cardioprotective substance. Ann. N. Y. Acad. Sci. 1215, 16–21. https://doi.org/10.1111/j.1749-6632.2010.05854.x. Jan.

Yáñez, J.A., Wang, S.W., Knemeyer, I.W., Wirth, M.A., KB, A., 2011. Intestinal lymphatic transport for drug delivery. Adv. Drug Deliv. Rev. 63 (10–11), 923–942. https://doi.org/10.1016/j.addr.2011.05.019. Sep 10.

Yuan, Z.X., Deng, S., Chen, L., Hu, Y., Gu, J., He, L., 2021. pH-driven entrapment of enrofloxacin in casein-based nanoparticles for the enhancement of oral bioavailability. Food Sci. Nutr. 9 (8), 4057–4067. https://doi.org/10.1002/fsn3.2224. Apr 7.

Zhang, Z., Lu, Yi., Qi, J., Wu. W. An update on oral drug delivery via intestinal lymphatic transport, 2024.

Zhu, Y., Ye, J., Zhang, Q., 2020. Self-emulsifying drug delivery system improve oral bioavailability: role of excipients and physico-chemical characterization. Pharm. Nanotechnol. 8 (4), 290–301. https://doi.org/10.2174/2211738508666200811104240.